OPEN ACCESS
IOP Publishing
Journal of Physics: Condensed Matter
J. Phys.: Condens. Matter **32** (2020) 165001 (5pp)
https://doi.org/10.1088/1361-648X/ab680c

Trivial band topology of ultra-thin rhombohedral Sb_2Se_3 grown on Bi_2Se_3

A V Matetskiy[1,2], V V Mararov[1], I A Kibirev[1], A V Zotov[1,2] and A A Saranin[1,2]

[1] Institute of Automation and Control Processes, Far Eastern Branch of RAS, Vladivostok 690041, Russia
[2] School of Natural Sciencies, Far Eastern Federal University, Vladivostok 690950, Russia

E-mail: mateckij@mail.dvo.ru

Received 17 October 2019, revised 2 December 2019
Accepted for publication 6 January 2020
Published 23 January 2020

Abstract

Thin films of rhombohedral Sb_2Se_3 with thicknesses from 1 to 5 quintuple layers (QL) were grown on Bi_2Se_3/Si(1 1 1) substrate. The electronic band structure of the grown films and the Sb_2Se_3/Bi_2Se_3 interface were studied using angle-resolved photoemission spectroscopy. It was found that while Sb_2Se_3 has an electronic band structure generally similar to that of Bi_2Se_3, there is no fingerprints of band inversion in it. Instead, the one-QL-thick Sb_2Se_3 films show direct band gap of about 80 meV. With growing film thickness, the Fermi level of the Sb_2Se_3 films gradually shifts by 200 meV for 5 QL-thick film revealing the band bending of the Sb_2Se_3/Bi_2Se_3 hetero-junction.

Keywords: topological insulator, heterostructure, electron photoemission

(Some figures may appear in colour only in the online journal)

1. Introduction

Nowadays, tetradymite family plays crucial role in a explosively growing field of topological states of matter. In particular, Bi_2Se_3, Bi_2Te_3 and Sb_2Te_3 have the same rhombohedral crystalline arrangement and similar inverted band structure with a descent gap of 0.2–0.3 eV [1]. As a result, their surfaces or interfaces with trivial insulators host conducting electronic states with helical spin texture. These unique topological surface states (TSS) define topological insulators (TI) as a perspective playground for observation of a variety spin-physics phenomena [2–4].

The above mentioned materials have a layered structure (figure 1(a)) where each so-called quintuple layer (QL) consists of alternating X-A-X-A-X atomic planes, where X is Se or Te and A–Bi or Sb. Within the layer, the atoms are covalently bonded, while layers are weakly bonded with each other via van der Waals (vdW) forces. Such structure allows precise control of the film thickness in the epitaxy process that can be used to tune the topological properties [5–7]. Moreover, using vdW epitaxy approach [8, 9], one can combine these topological insulators with other materials, that opens a way for observation such striking phenomena as quantum anomalous Hall effect [2] and Majorana or Weyl quasi-particles [10, 11].

Among the four members of the chalcogenide family with rhombohedral crystalline structure [1] only the Sb_2Se_3 stays unexplored. Bulk Sb_2Se_3 arranges in the orthorhombic phase with trivial insulator behavior and band gap of ~1.1 eV [12, 13]. However, *ab initio* calculations shows that rhombohedral structure of Sb_2Se_3 is kinetically stable [14]. In the experiments with the $(Bi_{(1-x)}Sb_x)_2Se_3$ thin films (15–25 QL), rhombohedral phase was found to be stable for x of up to 0.5 on Al_2O_3 substrate [15] and up to 0.7 on Bi_2Se_3 substrate [16]. Whether the rhombohedral Sb_2Se_3 phase has a band inversion or not appeared to depend on the calculation procedure [1, 14, 17, 18]. Furthermore, for the Sb_2Se_3/Bi_2Se_3 heterostructure, calculations predict penetration of the Bi_2Se_3 topological interface states through the slab of the trivial Sb_2Se_3 [18]. Motivated by these findings and existed discrepancy in the calculation results, we performed an experimental study of the crystalline and electronic band structures of the Sb_2Se_3 ultra-thin films (1–5 QL) grown on the thick Bi_2Se_3 buffer layer.

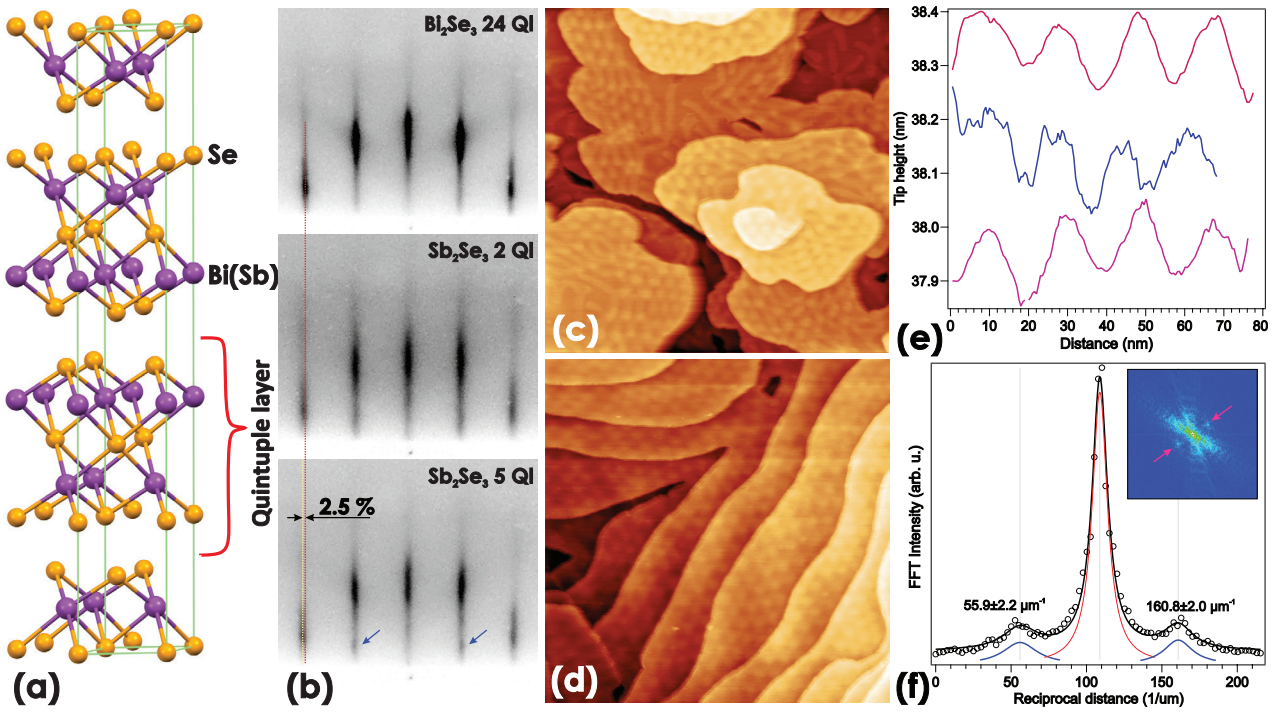

Figure 1. (a) Ball-and-stick model of the rhombohedral Bi_2Se_3 or Sb_2Se_3 crystals. Bismuth or antimony atoms are shown by purple balls, selenium atoms by yellow balls. (b) RHEED patterns from to the initial Bi_2Se_3 film of 24 QL thickness grown on Si(1 1 1) and Sb_2Se_3 2 QL and 5 QL-thick films grown atop of it. ((c) and (d)) STM images ($400 \times 400\,nm^2$, $V_s = -0.8$ V) of 2 and 5 QL-thick films of Sb_2Se_3 grown on Bi_2Se_3. (e) STM profiles along the hexagonal Moiré directions. Profiles are separated by 0.15 nm in height for clarity. (f) FFT image taken from (d) together with profile along line marked by red arrows. Profile is fitted by Lorentzians. Red peak corresponds to low frequency background while blue peaks correspond to Moiré lattice.

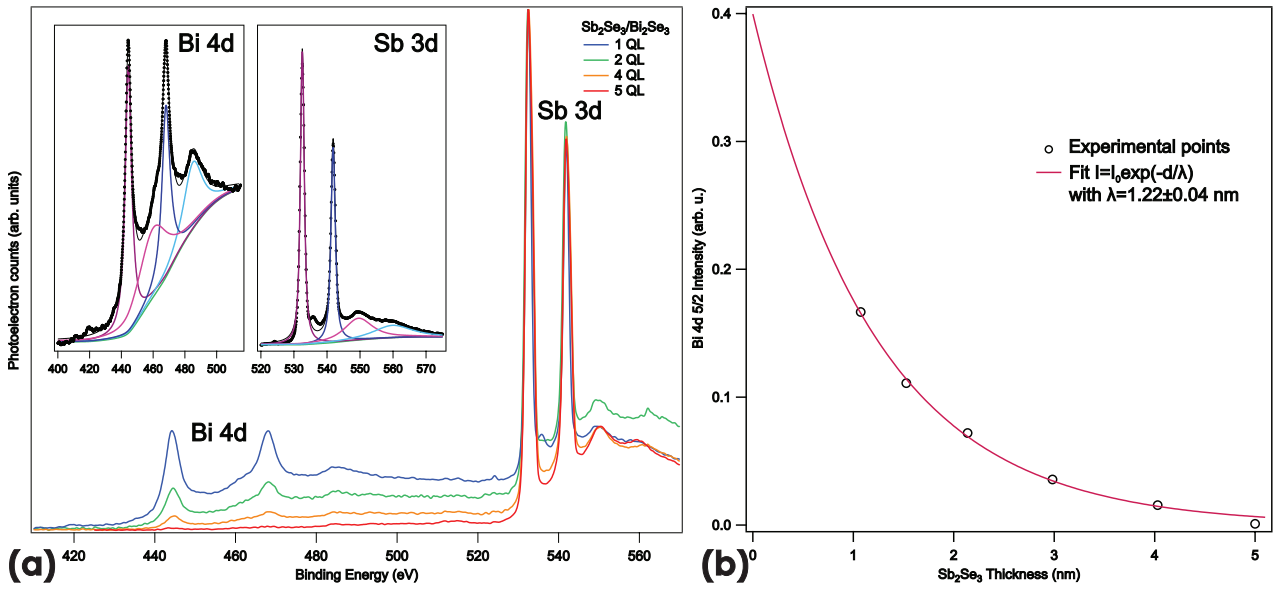

Figure 2. (a) XPS spectra from the Sb_2Se_3 films of various thicknesses (1, 2, 4 and 5 QL) grown on Bi_2Se_3 substrate. Fitting results for the Bi 4d and Sb 3d peaks of 1 QL-thick film are shown in the insets. Purple and blue peaks depict 5/2 and 3/2 lines, respectively, while pink and cyan depict corresponding shake-up satellites. Tougaard background is marked by green line. (b) Attenuation of the XPS intensity of the Bi 4d 5/2 peak as function of Sb_2Se_3 overlayer thickness.

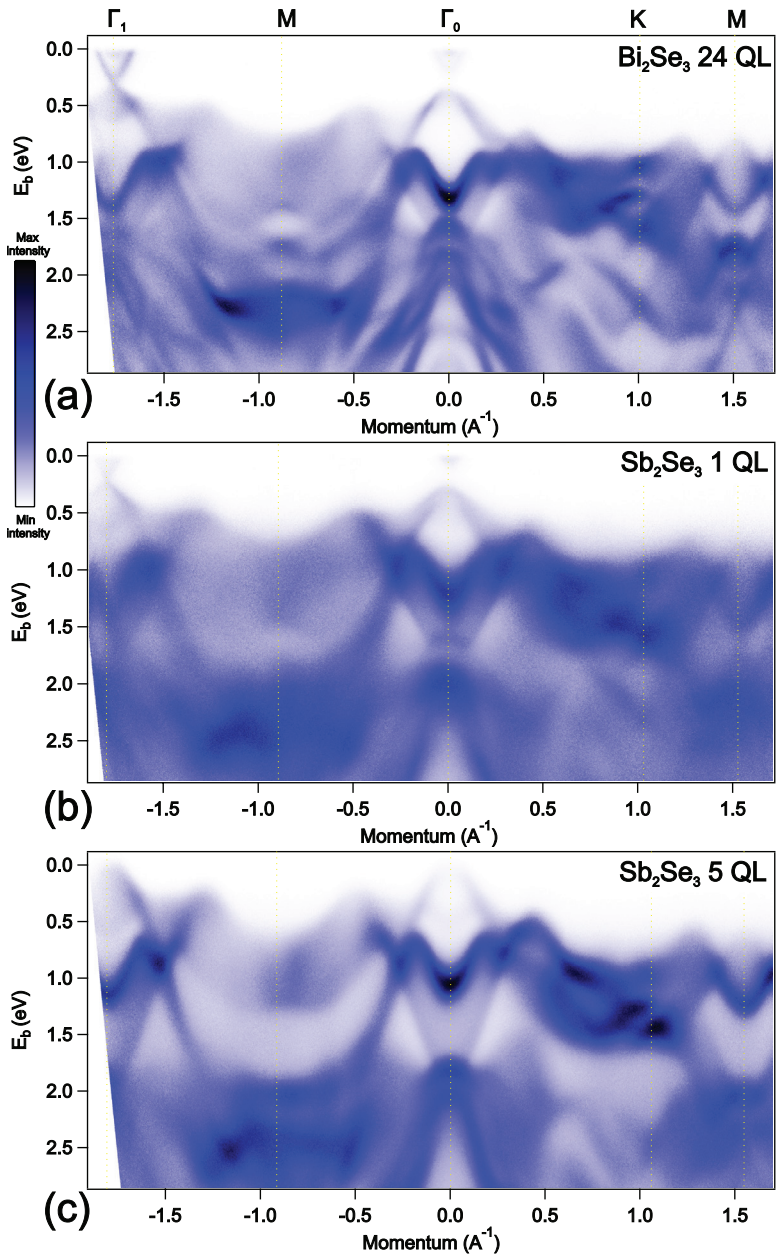

Figure 3. ARPES data along the Γ_1-M-Γ_0-K-M directions for (a) Bi_2Se_3 substrate and Sb_2Se_3 films with thickness of (b) 1 QL and (c) 5 QL grown on Bi_2Se_3.

2. Experimental details

In the present study, MBE growth of selenides was conducted in the ultrahigh vacuum (UHV) chamber with a base pressure less than 5.0×10^{-10} Torr, equipped with reflection-high-energy electron diffraction (RHEED) facility. Atomically-clean Si(1 1 1)7 × 7 surface was prepared *in situ* by flashing the Si(1 1 1) samples to 1280 °C after they were first outgassed at 600 °C for 6 h. Details of the Bi_2Se_3/Si(1 1 1) sample preparation could be found elsewhere [19]. Bismuth, antimony and selenium were deposited from the Knudsen cells heated to 470, 380 and 195 °C, respectively. Thus, the flux ratio of Bi (Sb) to Se was about 1:10. Growth rate of Sb_2Se_3 was about 0.5 QL min^{-1}. Substrate temperature during Sb_2Se_3 growth was about 170 °C. The prepared samples were transferred, using evacuated transfer unit, into the UHV Omicron MULTIPROBE system, equipped with scanning tunneling microscopy (STM), x-ray photoemission spectroscopy (XPS) and angle-resolved photoemission spectroscopy (ARPES) facilities. Spectroscopy measurements were conducted using VG Scienta R3000 electron analyzer, Mg x-ray source ($h\nu = 1253.7$ eV) and high-flux He discharge lamp ($h\nu = 21.2$ eV).

3. Results and discussion

Figure 1(b) shows RHEED patterns from the initial Bi_2Se_3 substrate and Sb_2Se_3 films of 2 QL and 5 QL thickness grown atop of it. It turns out that film preserves the crystal structure of the substrate for the thicknesses of up to 5 QL. There is a slight

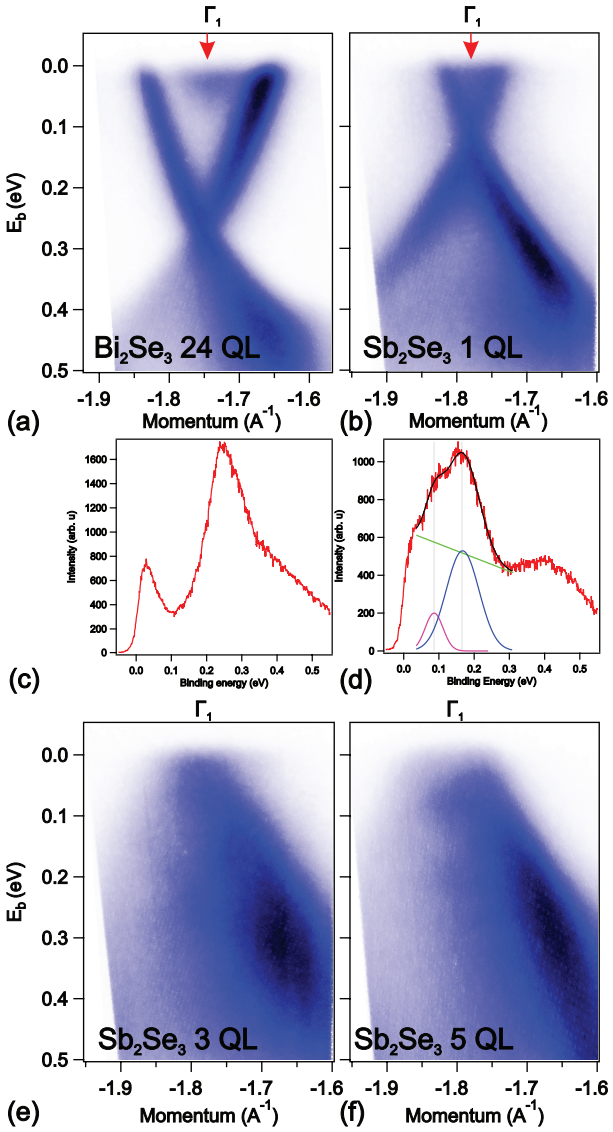

Figure 4. ARPES spectra in the Γ_1 point of the (a) initial 24 QL-thick Bi_2Se_3 and ((b), (e) and (f)) one-, three- and five-QL-thick Sb_2Se_3/Bi_2Se_3. Red arrows mark positions of the energy distribution curves (EDC) depicted below the spectra. ((c) and (d)) EDC taken at Γ_1 from (a) and (b), respectively. Curve in (d) is fitted by two Gaussians (pink and blue lines) with linear background (green line).

increase of reciprocal lattice constant of about 2.5%. Bearing in mind that lattice constant of thick Bi_2Se_3 film on Si(1 1 1) $\mathbf{a}_{Bi_2Se_3} = 4.147$ Å [20] one can obtain $\mathbf{a}_{Sb_2Se_3} = 4.048 \pm 0.003$ Å. For the 5 QL-thick Sb_2Se_3 film, one can notice faint additional spots marked by blue arrows. We attribute them to the islands of the orthorhombic phase that should be more stable for the thick films. Thus, rhombohedral Sb_2Se_3 is believed to persist in a relatively narrow region of the film thicknesses.

In the STM images (figures 1(c) and (d)), Sb_2Se_3 films exhibit morphology similar to that of the Bi_2Se_3 substrate with screw dislocations and steps of $\approx$1 nm height. One can also notice weakly periodic Moiré pattern that does not show long-range order. Moiré periodicity can be roughly estimate from the set of the STM profiles (figure 1(e)) which gives $\mathbf{A} = 19 \pm 2$ nm. Similar value can be obtained from the fast-Fourier-transform (FFT) profile (figure 1(f)) where Lorentzian fit gives $\mathbf{A} = 19.2 \pm 0.8$ nm.

Due to a low growth temperature of the Sb_2Se_3 films, we expect that diffusion of Bi atoms into the film is negligible. Observed Moiré pattern in the STM images also suggests that lattice constant changes stepwise after formation of the first Sb_2Se_3 layer and interface is sharp. This conclusion is supported by the results of the XPS measurements conducted for the Sb_2Se_3 films of various thicknesses (figure 2). Bismuth signal was found to decrease exponentially with the thickness and already vanishes for the 5 QL-thick film. Extracted inelastic mean free pass $\lambda = 1.22 \pm 0.04$ nm is in a agreement with universal curve value (1.54 nm) [21] for corresponded electron energy ($E_k = 810$ eV).

We will now discuss overall band structures and then take a close look on a Γ point. Figure 3 shows the ARPES data recorded along the main directions of surface Brillouin zone for the Bi_2Se_3 substrate and the Sb_2Se_3 films (1 and 5 QL). One can notice that film and the substrate have similar band structures. According to the calculations [1], in the crystals of Bi_2Se_3 family the highest valence band is mainly occupied by chalcogen p_z orbitals and the lowest conduction band is mainly occupied by Bi (Sb) p_z orbitals. Both calculated [1, 14, 18, 23] and experimental spectra for Sb_2Se_3 show valence band maximum (VBM) in the Γ point. In the ΓM direction the experimental dispersion of the highest valence band shows additional maximum that is $\sim$200 meV lower then VBM and minimum in M point that is $\sim$600 meV lower then VBM. Calculations [1, 14, 18, 23] show similar dispersion along ΓM with slightly closer position in energy of the additional maximum to VBM. In the ΓK direction the experimental dispersion of the highest valence band shows additional maximum that is $\sim$500 meV lower then VBM and then stays relatively flat until it reach the K point and show maximum in the middle of KM that is $\sim$500 meV lower then VBM. This particular behavior well coincide with one obtained in calculations by Liu *et al* [23] and contradicts with calculations by Cao *et al* [14] that show maximum in K point.

We will now consider the electron band structure in the vicinity of Γ point. As mentioned in the introduction, depending on the calculation procedure, numerical studies show topological trivial [1] and non-trivial [14] behavior for the rhombohedral Sb_2Se_3 as well as transition among these phases under the pressure [22, 23]. Figure 4 presents detailed spectroscopy data in the Γ point of Sb_2Se_3/Bi_2Se_3 system as a function of film thickness (measurements were done in the Γ_1 point instead of the Γ_0 point due to better resolution and positioning). As was shown by Zhang *et al* [1] strong spin–orbit interaction leads to inversion of orbital character near the Γ point for Bi_2Se_3, Bi_2Te_3 and Sb_2Te_3 and corresponded topological insulator behavior with gapless states on a surface. Indeed, on a spectrum of Bi_2Se_3 substrate one can see the conduction band touching the Fermi level and the Dirac cone of the topological surface states (figure 4(a)) with the position of the Dirac point at $\sim$240 meV. On energy distribution curve (EDC) in figure 4(c) the Dirac point appears as the spectral intensity maximum. On the the spectrum for the 1 QL-thick Sb_2Se_3 film (figure 4(b)), one can see conduction

and valence bands as two cones touching each other. Their apexes are separated by the tiny gap of about 79 ± 15 meV as one can see on a EDC curve fit in figure 4(d) where instead of single Dirac point maximum double peak feature appears. Similar gap size was predicted for bulk Sb_2Se_3 by Zhang *et al* [1] and Liu *et al* [23].

For this Sb_2Se_3/Bi_2Se_3 system the total thickness is 25 QL. In their comprehensive numerical study of the Bi_2Se_3 family heterostructures Aramberri and Muñoz [17] showed that in case of the topological insulator/topological insulator heterostructure (in their example, Sb_2Te_3/Bi_2Te_3) even if one of the topological insulators is below penetration depth of the TSS, there is no gap in the spectrum, as well as no interface states. Thus, topological insulator/topological insulator heterostructure acts as a whole in terms of coupling of bottom and top TSS. Similar picture was found in the experimental study of Sb_2Te_3/Bi_2Te_3 heterostructure [24]. In the current case of 1 QL-thick Sb_2Se_3 film on thick Bi_2Se_3, the observed gap supports trivial insulator behavior of the Sb_2Se_3.

With growing film thickness (figures 4(e) and (f)), the Sb_2Se_3 bands continuously shift to lower binding energy by 200 meV for the 5 QL-thick film with respect to the 1 QL-thick film. Thus, the Fermi level lies in the conduction band (electron-like dispersion) at lower thicknesses and in the valence band (hole-like dispersion) at higher thicknesses with position inside the gap for 3 QL-thick film. While electron doping of Bi_2Se_3 usually is explained by Se vacancies, slight hole doping of the Sb_2Se_3 can be explained by formation of Sb vacancies in analogy with the Sb_2Te_3 case [25]. This leads to p-n junction formation and corresponded band alignment observed in the ARPES measurements. A similar trend was observed for $(Bi_{1-x}Sb_x)_2Se_3/Bi_2Se_3$ heterostructures [16].

4. Conclusions

The goal of this study was to clarify experimentally the electronic and topological properties of the rhombohedral Sb_2Se_3 and Sb_2Se_3/Bi_2Se_3 interface. While we did succeed in growing the rhombohedral Sb_2Se_3 phase on Bi_2Se_3 substrate, we did not find any fingerprints of its non-trivial topology. Instead, 1 QL-thick Sb_2Se_3 film grown on 24 QL-thick Bi_2Se_3 substrate shows trivial gap of about 80 meV, which is unlikely for topological insulator/topological insulator heterostructure [16, 17]. Observation of the gap also contradicts the predicted penetration of the Bi_2Se_3 topological interface states through the slab of the trivial Sb_2Se_3 [18]. In calculations [17], the Sb_2Se_3 topological-insulator phase was found to realize in a narrow region of lattice parameters. Thus, a principal possibility to realize Sb_2Se_3 topological-insulator phase still remains choosing an appropriate substrate, provided that orthorhombic phase issue would be satisfied. The present experimental results on the electronic band structure of the rhombohedral Sb_2Se_3 phase could help for future studies of its family.

Acknowledgments

The present work was supported in part by the Grant MK-4472.2018.2 of the President of the Russian Federation and the Grant 19-02-00549 A of the Russian Foundation for Basic Research.

ORCID iDs

A V Matetskiy https://orcid.org/0000-0002-4967-604X
A A Saranin https://orcid.org/0000-0001-6642-2466

References

[1] Zhang H, Liu C X, Qi X L, Dai X, Fang Z and Zhang S C 2009 *Nat. Phys.* **5** 438–42
[2] Hasan M Z and Kane C L 2010 *Rev. Mod. Phys.* **82** 3045–67
[3] Ando Y 2013 *J. Phys. Soc. Japan* **82** 102001
[4] Qi X L and Zhang S C 2011 *Rev. Mod. Phys.* **83** 1057–110
[5] Zhang Y *et al* 2010 *Nat. Phys.* **6** 584–8
[6] Liu Y, Bian G, Miller T, Bissen M and Chiang T C 2012 *Phys. Rev.* B **85** 195442
[7] Förster T, Krüger P and Rohlfing M 2016 *Phys. Rev.* B **93** 205442
[8] Koma A and Yoshimura K 1986 *Surf. Sci. Lett.* **174** A459
[9] Geim A K and Grigorieva I V 2013 *Nature* **499** 419–25
[10] Fu L and Kane C L 2008 *Phys. Rev. Lett.* **100** 096407
[11] Burkov A A and Balents L 2011 *Phys. Rev. Lett.* **107** 127205
[12] Kosek F, Tulka J and Štourač L 1978 *Czechosl. J. Phys.* B **28** 325–30
[13] Koc H, Mamedov A M, Deligoz E and Ozisik H 2012 *Solid State Sci.* **14** 1211–20
[14] Cao G, Liu H, Liang J, Cheng L, Fan D and Zhang Z 2018 *Phys. Rev.* B **97** 075147
[15] Liu Y, Chong C, Chen W, Huang J A, Cheng C, Tsuei K, Li Z, Qiu H and Marchenkov V V 2017 *Japan. J. Appl. Phys.* **56** 070311
[16] Satake Y, Shiogai J, Takane D, Yamada K, Fujiwara K, Souma S, Sato T, Takahashi T and Tsukazaki A 2018 *J. Phys.: Condens. Matter* **30** 085501
[17] Aramberri H and Muñoz M C 2017 *Phys. Rev.* B **95** 205422
[18] Zhang Q, Zhang Z, Zhu Z, Schwingenschlögl U and Cui Y 2012 *ACS Nano* **6** 2345–52
[19] Matetskiy A V, Kibirev I A, Hirahara T, Hasegawa S, Zotov A V and Saranin A A 2015 *Appl. Phys. Lett.* **107** 091604
[20] Vyshnepolsky M, Klein C, Klasing F, Hanisch-Blicharski A and Horn-von Hoegen M 2013 *Appl. Phys. Lett.* **103** 111909
[21] Seah M P and Dench W A 1979 *Surf. Interface Anal.* **1** 2–11
[22] Li W, Wei X Y, Zhu J X, Ting C S and Chen Y 2014 *Phys. Rev.* B **89** 035101
[23] Liu W, Peng X, Tang C, Sun L, Zhang K and Zhong J 2011 *Phys. Rev.* B **84** 245105
[24] Eschbach M *et al* 2015 *Nat. Commun.* **6** 8816
[25] Jiang Y *et al* 2012 *Phys. Rev. Lett.* **108** 066809